Low-energy ^{18}F(p, α)^{15}O cross section measurements relevant to nova γ-ray emission

N. de Séréville,[1,2,*] C. Angulo,[1,†] A. Coc,[3] N. L. Achouri,[4] E. Casarejos,[5] T. Davinson,[6] P. Descouvemont,[7] P. Figuera,[8] S. Fox,[9] F. Hammache,[2] J. Kiener,[3] A. Laird,[9] A. Lefebvre-Schuhl,[3] P. Leleux,[1] P. Mumby-Croft,[9] N. A. Orr,[4] I. Stefan,[2,10] K. Vaughan,[9] and V. Tatischeff[3]

[1]*CRC and IPN, Université catholique de Louvain, B-1348 Louvain-la-Neuve, Belgium*
[2]*IPN, IN2P3-CNRS et Université Paris Sud, F-91406 Orsay Cedex, France*
[3]*CSNSM, IN2P3-CNRS et Université Paris Sud, F-91405 Orsay campus, France*
[4]*LPC-ENSICAEN, IN2P3-CNRS et Université de Caen, F-14050 Caen Cedex, France*
[5]*Universidad de Santiago de Compostela, E-15782 Santiago de Compostela, Spain*
[6]*School of Physics, University of Edinburgh, Edinburgh EH9 3JZ, United Kingdom*
[7]*PNTPM, CP229, Université Libre de Bruxelles, B-1050 Brussels, Belgium*
[8]*Laboratori Nazionali del Sud, INFN, Via S. Sofia 44, I-95123 Catania, Italy*
[9]*Department of Physics, University of York, Heslington, York YO10 5DD, United Kingdom*
[10]*GANIL, B.P. 5027, F-14021 Caen Cedex, France*

(Received 27 November 2007; revised manuscript received 29 October 2008; published 9 January 2009)

During nova outbursts the decay of ^{18}F is the main source of γ-ray emission at and below 511 keV. In spite of much experimental effort, the quantity of ^{18}F synthesized still suffers from large uncertainties which arise mainly from the ^{18}F(p, α)^{15}O reaction cross section at low energies. We report here on a new direct measurement carried out at the Louvain-la-Neuve RIB facility of Louvain-la-Neuve using an isobarically pure ^{18}F beam impinging on a thin polyethylene target. Cross sections down to a center-of-mass energy of 400 keV have been obtained and the results together with previous experimental data were compared to $\mathcal{R}$-matrix calculations. The effect of the relative contribution of the two low-lying $3/2^+$ resonances as well as the sensitivity of the calculations to the $\mathcal{R}$-matrix radius is studied in detail.

DOI: 10.1103/PhysRevC.79.015801 PACS number(s): 25.60.Je, 21.10.Jx, 26.30.Ca, 27.20.+n

I. INTRODUCTION

Gamma-ray emission from classical novae is dominated during the first hours by positron annihilation following the β^+ decay of radioactive nuclei. The main contribution arises from the decay of ^{18}F (half-life 110 min) and hence is directly related to the formation of ^{18}F during the outburst [1–3]. This is of special interest since this γ-ray emission could be detected with satellite missions, such as INTEGRAL, or future γ-ray telescopes. A good understanding of the nuclear reaction rates producing and depleting ^{18}F is required to calculate the quantity of ^{18}F synthesized in novae and the resulting gamma-ray emission at and below 511 keV. In the following we focus on the destruction of ^{18}F via the reaction ^{18}F(p, α)^{15}O, the rate of which still remains highly uncertain.

The calculation of the rate involves several resonances in the ^{19}Ne compound nucleus within 1 MeV of the proton threshold. Apart from a $3/2^-$ resonance ($E_r = 330$ keV), most of the resonances involved are $3/2^+$. One of them is the $E_r = 665$ keV resonance which has been extensively studied in the past [4–9] and for which the properties (Γ_p, Γ_α, $\Gamma_{\rm tot}$) are now well established. Owing to its large total width ($\Gamma_{\rm tot} =$ 40 keV) it contributes significantly to the reaction rate. At much lower energy and closer to the proton threshold, the proton widths of two $3/2^+$ resonances ($E_r = 8$ and 38 keV) have been recently determined through the study of their analog levels in the mirror nucleus ^{19}F [10,11]. Uncertainties in the properties of these two resonances and their impact on the reaction rate have been presented elsewhere [12]. The most important effect comes from interference between the low-lying and high-energy resonances the signs of which are totally unknown and which contribute to the cross section mostly in the Gamow peak region.

We report here on a direct measurement of the ^{18}F(p, α)^{15}O reaction at four different energies in the range $E_{\rm c.m.} =$ 400–700 keV with the goal of constraining the sign of the interference between the $3/2^+$ resonances. Two measurements were performed in the region of the $E_r = 665$ keV resonance for normalization purposes whereas the other two measurements were performed at lower energies corresponding to the tail of this resonance where the interference effects are most important. In the first part of this paper we present the experimental method followed by a description of the data analysis. In the second part of this paper, the $\mathcal{R}$-matrix analysis of the cross section is presented.

II. EXPERIMENTAL METHOD

The experiment was performed at the Centre de Recherches du Cyclotron, UCL, Louvain-la-Neuve, Belgium. The 13.8 MeV ^{18}F radioactive beam was produced via the ^{18}O(p, n)^{18}F reaction, chemically extracted to form $CH_3{}^{18}F$ molecules, transferred to an ECR source, ionized to the 2^+ state, and then accelerated [13]. The ^{18}F production was

*deserevi@ipno.in2p3.fr
†Present address: Tractebel Engineering (SUEZ), Av. Ariane 7, B-1200 Brussels, Belgium.

performed in a batch mode and an average of 1.0×10^6 ^{18}F ions per second on target was delivered for a total of 50 h. The beam bombarded a 70 μg/cm^2 polyethylene (CH_2) target and the products of the ^{18}F$(p,\alpha)^{15}$O reaction were detected using two 300 μm thick silicon strip LEDA detectors [14] made up of eight sectors, each divided into 16 radial strips of 5 mm width.

The α particles from the ^{18}F$(p,\alpha)^{15}$O reaction were detected in the first LEDA detector (LEDA1) positioned 8.5 cm downstream from the target and covering laboratory angles between 30.5° and 56.8°. Owing to the properties of inverse kinematics, the ^{15}O nuclei were emitted in a forward cone out to $\theta = 23°$ in the laboratory. The second LEDA detector (LEDA2) was thus positioned 32 cm downstream from the target covering the laboratory angles between 8.9° and 22.1°. The positioning of the detectors was optimized on the basis of Monte Carlo simulations: for LEDA1, the angular range and detection efficiency were maximized and for LEDA2, the coincidence efficiency between α particles and ^{15}O was optimized.

As noted above, the ^{18}F$(p,\alpha)^{15}$O cross section was measured at four different laboratory energies. In order to vary the beam energy without the very time consuming procedure of retuning the cyclotron, aluminium degrader foils were employed. Foils of 95, 500, and 670 μg/cm^2 thickness were used, corresponding to ^{18}F energies on target of 13.1, 9.9, and 8.6 MeV, respectively. At low energy, the energy and spot size of the beam were not as good as at higher energy owing to the straggling induced by the degraders. However, in the present experiment the energy resolution was not crucial since the cross section does not exhibit narrow resonances and only a determination of the number of $\alpha + ^{15}$O coincidence events was required.

In order to check the beam properties (in particular the beam energy) after each degrader, a calibrated 1 cm^2 silicon PIPS (passivated implanted planar detector) detector of 300 μm thickness placed at zero degrees downstream from the target was used. The mean energy and the energy profile of the beam were measured; this allowed the degrader thicknesses to be verified (they were found to be within 10% of their nominal values). In addition, by comparing the difference in energy loss between ^{18}F and ^{18}O in the 670 μg/cm^2 aluminium foil, it was possible to determine the beam purity—the stable isobar ^{18}O being the principal impurity—^{18}O / ^{18}F $< 0.5\%$ (see Ref. [15] for more details).

The data were collected in event-by-event mode whereby the multiplicity, angle, deposited energy, and time of flight measured relative to the cyclotron radio-frequency were recorded, allowing an off-line analysis of single and coincidence events. The energy calibration of the two LEDA detectors was performed using a calibrated 3α-source (^{239}Pu, ^{241}Am, and ^{244}Cm) whereas the time-of-flight calibration was performed using a precision pulse generator.

III. DATA ANALYSIS

A. Data reduction

The coincidence spectra obtained on the $E_r = 665$ keV resonance with the 95 μg/cm^2 aluminium degrader are shown in Fig. 1(top). The coincidence condition between the two LEDA detectors allows the events from the ^{18}F$(p,\alpha)^{15}$O reaction to be readily identified in the (E_1, E_2) spectrum (Fig. 1 top left). The correlation observed between the registered energies in the two LEDA detectors is characteristic of a two-body reaction and was, after reconstructing the Q-value, identified as the ^{18}F$(p,\alpha)^{15}$O reaction. The same coincidence events are displayed in a (E,θ) spectrum for LEDA1 (Fig. 1 top middle) where the kinematical band corresponding to α particles is clearly observed. The events with E(LEDA1) < 2 MeV correspond to ^{18}F + ^{12}C elastic scattering. A full Monte Carlo simulation of the experimental setup, including energy losses in the degrader and the target, as well as the spatial and energy resolution of the beam, was performed and a very good agreement with these two spectra was observed. This further reinforced the identification of the events as arising from the ^{18}F$(p,\alpha)^{15}$O reaction. Selection of the ^{18}F$(p,\alpha)^{15}$O events in the (E_1, E_2) spectrum gives some 1400 and 4100 events for the beam energies of 13.8 and 13.1 MeV, respectively.

As noted earlier, in order to be sensitive to the interference between the various $3/2^+$ resonances, the ^{18}F$(p,\alpha)^{15}$O cross section was measured in the low-energy tail of the $E_r = 665$ keV resonance at beam energies of $E_{\rm lab} = 9.9$ and 8.6 MeV. In this case, the selection of the coincidence events is somewhat more difficult as the ^{18}F$(p,\alpha)^{15}$O cross section is decreasing owing to the Coulomb penetrability, while the ^{18}F + ^{12}C elastic scattering cross section increases at the lower center-of-mass energies. The α-^{15}O coincidence events are thus no longer well separated from the ^{18}F + ^{12}C elastic scattering events in the (E_1, E_2) spectrum (Fig. 1 bottom left). However, as the α particles were well identified in the (E_1, θ_1) spectrum an additional condition was applied along this kinematical band (Fig. 1 bottom middle). As a result, 180 and 39 α-^{15}O coincidence events were identified (Fig. 1 bottom right) at $E_{\rm lab} = 9.9$ and 8.6 MeV, respectively. Background measurements with a pure carbon target as well as with an empty target frame were also run. In both cases, no coincidence events were observed in the region of interest.

B. Cross section

The total cross section in the center-of-mass system was calculated from the observed yield at each energy following the relation:

$$\sigma(E) = \frac{1}{I N_p} \sum_s \left(\frac{Y_s(E)}{\Delta\Omega_s \epsilon_s} \right) \times 4\pi,$$

where I is the number of incident ^{18}F ions and N_p the proton content of the target per unit area. The sum was performed over the 16 strips s of the LEDA1 detector, where $Y_s(E)$ was the number of α particles detected from the ^{18}F$(p,\alpha)^{15}$O reaction in a given strip in coincidence with ^{15}O ions, $\Delta\Omega_s$ is the geometrical solid angle subtended by the strip in the center-of-mass and ϵ_s is the coincidence efficiency. The coincidence efficiency was determined from Monte Carlo simulations considering an isotropic angular distribution in the center-of-mass. Indeed this is what is observed in the data

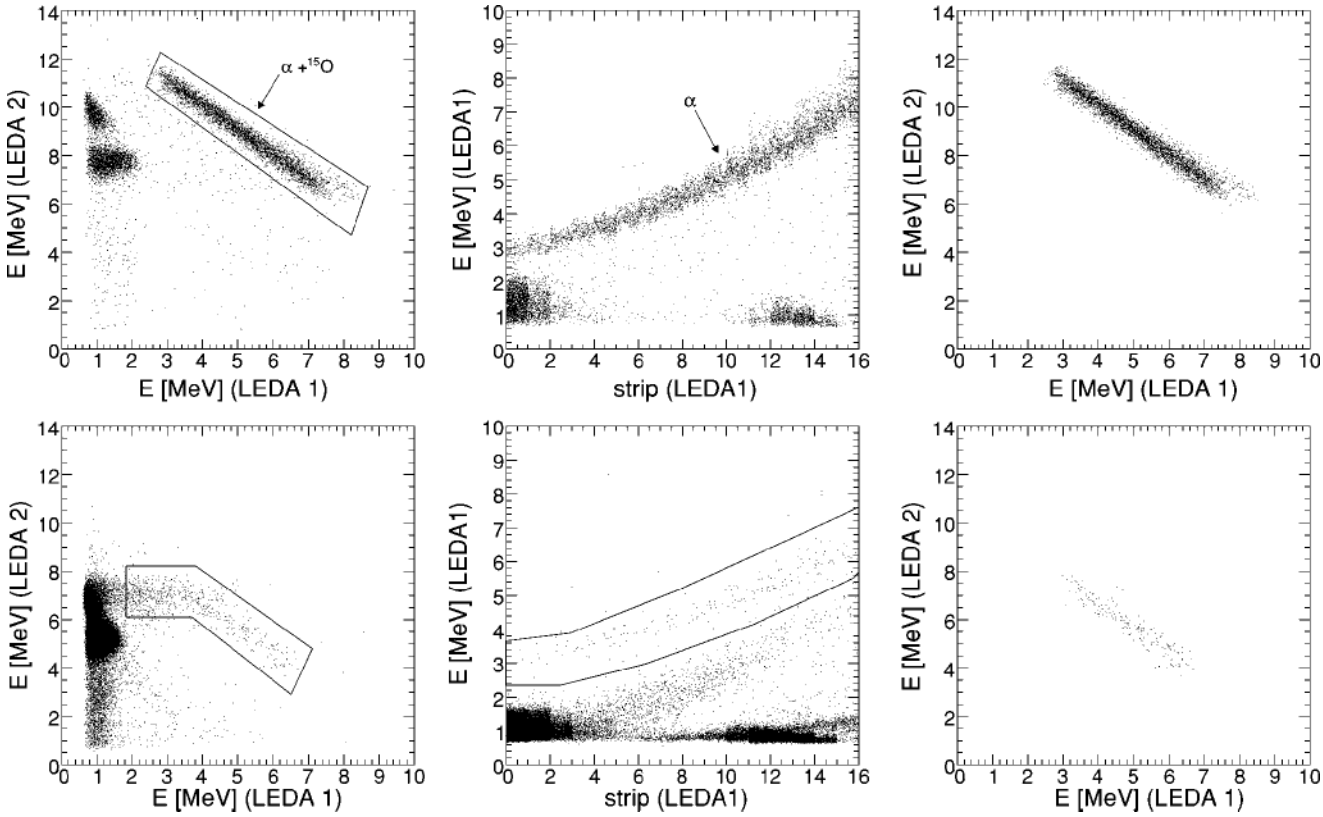

FIG. 1. Coincidence spectra on resonance for $E_{\rm lab} = 13.1$ MeV (95 μg/cm^2 degrader) (top) and off resonance for $E_{\rm lab} = 9.9$ MeV (500 μg/cm^2 degrader) (bottom). The conditions used to determine the number of α-^{15}O coincidences are shown in the left and middle panels: (E_1, E_2) and (E_1, θ_1) spectra, respectively. The right hand panels show the events after the conditions have been applied.

both "on" and "off" the $E_r = 665$ keV resonance as shown in Fig. 2.

The number of incident ^{18}F ions was determined from the ^{18}F + ^{12}C elastic scattering events detected in LEDA2 in the eight strips at 19.4°, which have the largest solid angle and which are the least sensitive to the exact position of the beam on target. Furthermore, the elastic scattering peaks of ^{18}F and ^{12}C are well separated in the time-of-flight versus energy spectrum.

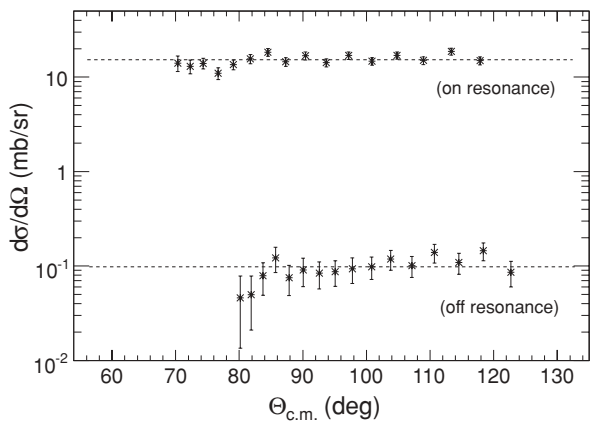

FIG. 2. Differential cross section for the ^{18}F(p, α)^{15}O reaction "on" ($E_{\rm lab} = 13.8$ MeV) and "off" ($E_{\rm lab} = 9.9$ MeV) resonance. The dashed lines represent the mean value of the differential cross section.

As the beam intensity was deduced from elastic scattering on the ^{12}C content of the target and the ^{18}F(p, α)^{15}O cross section depends on the hydrogen content of the target, the normalization does not depend on the target thickness but on the target stoichiometry. This quantity was determined from the cross section of the ^{1}H(^{18}O, α)^{15}N reaction, data for which were also acquired here. The data obtained without degrader ($E_{\rm c.m.} = 694$ keV) was used as at this energy the ^{1}H(^{18}O, α)^{15}N cross section is isotropic [16]. However, as this cross section is uncertain by 15% [17], the same uncertainty applies to the normalization of the ^{18}F(p, α)^{15}O cross section. The hydrogen content of the target was monitored during the experiment by checking the ratio of the number of protons and ^{12}C elastically scattered. No hydrogen depletion was observed as was expected given the low intensity of the ^{18}F beam.

The ^{18}F(p, α)^{15}O cross section deduced from the present measurement is reported in Fig. 3 along with earlier works [8,18]. Solid and dashed lines are $\mathcal{R}$-matrix calculation for the $E_r = 665$ keV resonance taking into account the target thickness effects corresponding to each experiment. This effect was simulated by the convolution of the cross section with a Gaussian of $\sigma = 16.5$ keV and 8.5 keV corresponding to target thicknesses of 70 μg/cm^2 and 35 μg/cm^2 used in the present and earlier works, respectively. Good agreement is observed between the different experimental data sets both in terms of the energy dependence and absolute values. For the present data, the error bars arise primarily from statistical

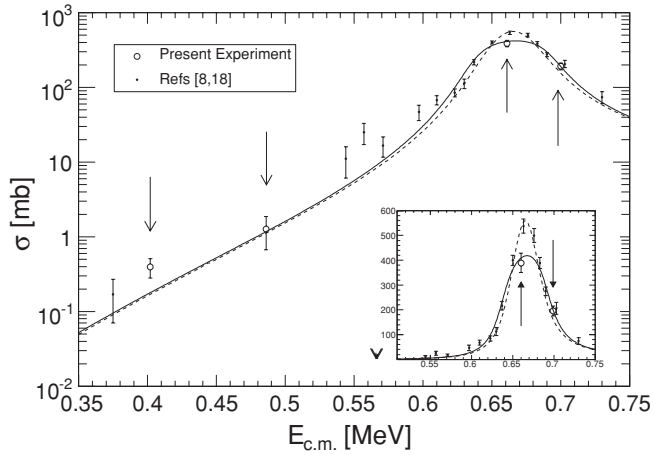

FIG. 3. Cross section of the ^{18}F$(p,\alpha)^{15}$O reaction as a function of the energy in the center of mass. The present (previous) experimental data are represented with open circles (dots) and vertical arrows. Solid and dashed lines are $\mathcal{R}$-matrix calculation for the $E_r = 665$ keV resonance taking into account the target thickness (see text). The inset shows the same data in linear scale focused around the resonance energy.

and coincidence efficiency uncertainties. Each data point is plotted at the center-of-mass energy corresponding to the beam energy at the target midpoint. Each measurement is an averaged cross section taken over the beam energy loss in the target (about 50 keV in the center-of-mass). For the two lowest energy points this effect was taken into account as an additional uncertainty which was added quadratically to the aforementioned uncertainties. This results in a smaller uncertainty at the lowest energy as the rate of change in the cross section with energy is smaller in the low energy tail of the resonance. The cross sections for the lowest energy data points at $E_{\mathrm{c.m.}} = 486$ and 402 keV are $\sigma = 1.26 \pm 0.59$ mb and 0.39 ± 0.11 mb, respectively.

IV. $\mathcal{R}$-MATRIX CALCULATIONS AND REACTION RATE

The ^{18}F$(p,\alpha)^{15}$O cross sections obtained here have been analyzed using an $\mathcal{R}$-matrix approach where the cross section is expressed as

$$\sigma(E) = \frac{\pi}{k^2} \sum_{J\pi} \frac{(2J+1)}{(2I_p+1)(2I_F+1)} \left|U^{J\pi}_{\alpha p}(E)\right|^2, \qquad (1)$$

where k is the wave number and $I_p = 1/2$ and $I_F = 1$ are the proton and ^{18}F spins. In general the sum is performed over all spins and parities but in the present case this is limited to the $J^\pi = 3/2^+$ resonances. $U^{J\pi}$ is the collision matrix which is determined in the $\mathcal{R}$-matrix formalism [19] from the R-matrix,

$$R^{J\pi}_{ij}(E) = \sum_{\lambda=1}^{N} \frac{\gamma^\lambda_i \gamma^\lambda_j}{E_\lambda - E}, \qquad (2)$$

where E_λ are the pole energies and γ^λ_i the reduced widths in channel i. For elastic scattering ($i = j$) the signs of γ^λ_i do not play a role, however they should be considered for transfer or inelastic processes. In the present case where interferences between several levels are taken into account each interfering level has a relative sign denoted "+" or "–" related to the sign of γ^λ_i. The product of the relative sign of two resonances determines the interference type: constructive or destructive. In the following, all the $\mathcal{R}$-matrix calculations were performed with the adopted value of 5.5 fm for the $\mathcal{R}$-matrix radius. The influence of the radius on the results is discussed later.

TABLE I. Spectroscopic information for the $3/2^+$ resonances of interest in ^{19}Ne (see text).

E_x [MeV]	E_r [keV]	Γ_p [keV]	Γ_α [keV]	Γ_γ [eV]	Refs.
6.419	8	$(0-3.4)\times10^{-37}$[a]	0.5	0.85	[22]
6.449	38	$(1.9-0)\times10^{-14}$[a]	1.2	1.2	[22]
7.076	665	15.4	23.8	1	[8]
7.238	827	0.35	6	1	[23]

[a]The exact value of the proton width depends on how the total proton spectroscopic factor is shared between the $E_r = 8$ and 38 keV resonances. Minimum and maximum values are given, corresponding to values of λ equal to 0 and 1, respectively (see text).

Four $3/2^+$ levels were considered in the present analysis as listed in Table I. Owing to its large total width the $E_r = 665$ keV resonance can interfere with the high-energy resonance at $E_r = 827$ keV and with the two low-lying resonances at $E_r = 8$ and 38 keV. Other resonances within 1 MeV of the proton threshold with different spin and parity are present in ^{19}Ne, however they have small total widths and cannot interfere with the $3/2^+$ resonances. Also a broad $1/2^+$ resonance was predicted more than 1 MeV above the proton threshold based on charge symmetry considerations [20] and has been recently observed. However, its contribution in the energy range of the present measurement was found to be unimportant [21]. These resonances were, therefore, not considered at this stage of the analysis.

Full $\mathcal{R}$-matrix calculations should take into account all $3/2^+$ resonances at the same time. However, a study of the interference between a pair of resonances is useful to estimate the impact of a given resonance. Calculations of the interference between the $E_r = 665$ and 827 keV resonances are shown in Fig. 4. The calculations have been convoluted with a target thickness of 70 μg/cm^2 corresponding to the experimental conditions of Ref. [24]. A negligible impact on the S-factor in the energy range of interest for novae outbursts ($E_{\mathrm{c.m.}} < 400$ keV) is observed, independent of the interference sign between the resonances at $E_r = 665$ and 827 keV. Hence, in the following discussion only the $E_r = 8$, 38, and 665 keV resonances were considered to have an impact in the energy range relevant for novae nucleosynthesis.

As far as the two lowest-lying resonances are concerned, their relative contributions are not well established. Indeed, the only available spectroscopic information is the total proton spectroscopic factor for this doublet as deduced from a study of the $d(^{18}\mathrm{F}, p)^{19}$F reaction [11,22]. Owing to the very small energy difference between these states the identification with analog levels in ^{19}Ne is not straightforward but there is a consensus that one of the two levels dominates [11,22] in

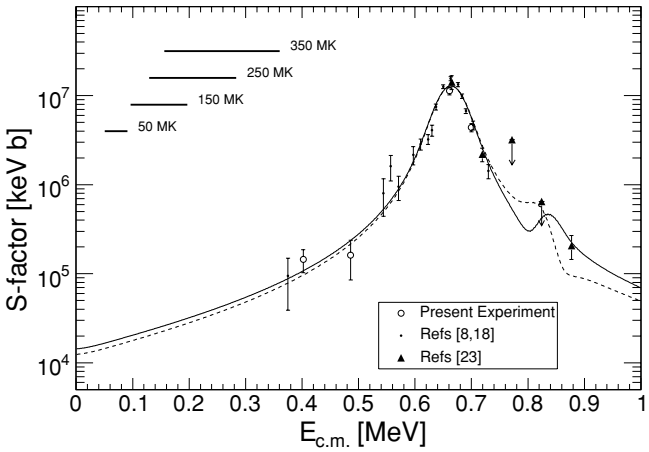

FIG. 4. Astrophysical S-factor for the ^{18}F$(p,\alpha)^{15}$O reaction. Same as Fig. 3 for the experimental data except above 750 keV in the center-of-mass which comes from [24]. Solid (dashed) lines are $\mathcal{R}$-matrix calculations for destructive (constructive) interference between the $E_r = 665$ and 827 keV resonances. The calculations take into account the effect of a target thickness of 70 μg/cm^2 [24]. The horizontal lines correspond to the Gamow peak calculated for several temperatures in novae.

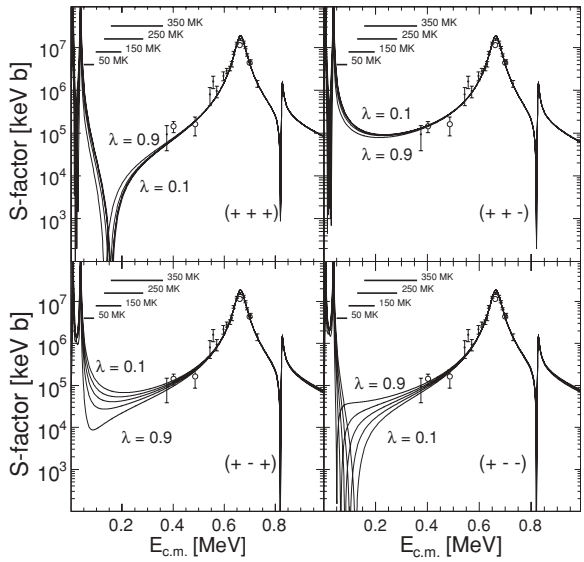

FIG. 5. Astrophysical S-factor for each interference type (labeled with the relative sign of each involved resonance). Experimental data as well as $\mathcal{R}$-matrix calculations for several values of the λ parameter are shown.

the $d(^{18}\mathrm{F},\ p)^{19}$F reaction. In the following several cases were computed corresponding to different relative populations of these two resonances. This was achieved by introducing the parameter λ which was defined as $\Gamma_p(8\ \mathrm{keV}) = \lambda\Gamma_p^0(8\ \mathrm{keV})$ and $\Gamma_p(38\ \mathrm{keV}) = [1-\lambda]\Gamma_p^0(38\ \mathrm{keV})$, where $\Gamma_p^0(8\ \mathrm{keV})$ and $\Gamma_p^0(38\ \mathrm{keV})$ correspond to the maximum values of the proton widths given in Table I. Small (large) values of the λ parameter favor a dominant contribution of the $E_r = 38$ keV (8 keV) resonance. The λ parameter was varied in steps of 0.1, however, as discussed above, only values close to 0 or 1 have a physical meaning. For each λ value $\mathcal{R}$-matrix calculations taking into account the $E_r = 665$ and 827 keV resonances were performed assuming a destructive interference between these two resonances.

Among the four $3/2^+$ resonances involved, as only three have unknown relative signs, eight different interference combinations are possible but since the global phase of the wave function is arbitrary the number of sign combinations is limited to four. The results are plotted in Fig. 5 where each panel represents an interference case labeled with three signs representing the relative sign of each interfering level. $\mathcal{R}$-matrix calculations corresponding to $\lambda = 0.1, 0.3, 0.5, 0.7,$ and 0.9 are displayed. One observes that two cases of interference corresponding to a destructive interference between the $E_r = 8$ and 38 keV resonances [(+ + +) and (+ + −)] are almost insensitive to the λ parameter. Hence, for these two cases the precise knowledge of the relative contribution of the two low-lying resonances is not crucial in order to determine the reaction rate. The two other cases corresponding to constructive interference between the $E_r = 8$ and 38 keV resonances [(+ − +) and (+ − −)] exhibit a much stronger dependence on the λ parameter. In these cases, the determination of the λ parameter is of special interest.

The calculations presented in Fig. 5 used a value for the $\mathcal{R}$-matrix radius of $a = 5.5$ fm. To illustrate the sensitivity of the calculations to the $\mathcal{R}$-matrix radius, three sets of calculations with $a = 4.5$, 5.5, and 6.5 fm for the case $\lambda = 0.2$ were performed (Fig. 6). One can observe that the most important effect is in the cases of the destructive interference [(+ − −) or (+ + +)] between the $E_r = 38$ and 665 keV resonances with respect to the cases of constructive interference [(+ − +) or (+ + −)] between these two resonances. The high sensitivity of the results in case of destructive interference arises from the cancellation of nondiagonal terms in Eq. (2). This dependence

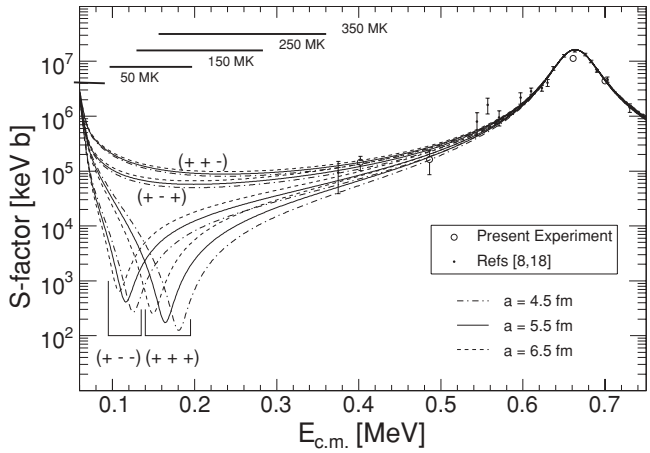

FIG. 6. Effect of the radius on the astrophysical S-factor for the ^{18}F$(p,\alpha)^{15}$O reaction for the special case of interference $\lambda = 0.2$. For each interference case calculations have been performed with three different values of the radius $a = 4.5$, 5.5, and 6.5 fm. All $\mathcal{R}$-matrix calculations take into account the effect of a target thickness of 35 μg/cm^2 [8].

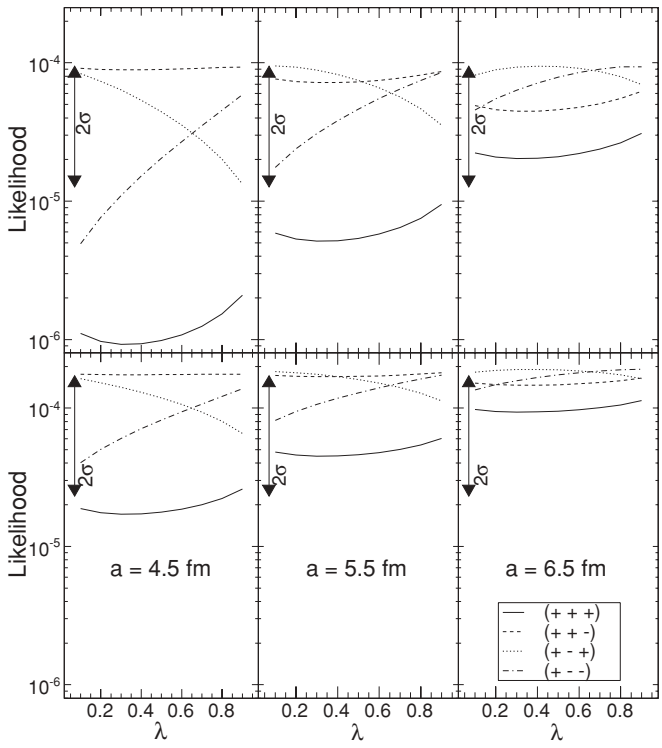

FIG. 7. Likelihood function for the four cases of interference between the $E_r = 8$, 38, and 665 keV resonances as a function of the λ parameter (see text). Top: Present and previous experimental data are taken into account. Bottom: Only previous experimental data are used. Results for three different radii $a = 4.5$, 5.5, and 6.5 fm are shown and the vertical arrow represents the confidence 2σ limit.

adds a further complexity level to the ^{18}F$(p,\alpha)^{15}$O reaction especially when destructive interferences are considered.

Comparison between the available data (present and previous experimental work) and $\mathcal{R}$-matrix calculations should then be done by taking carefully into account both the λ parameter and the $\mathcal{R}$-matrix radius effects. For each interference case the likelihood function ($\mathcal{L}$) was calculated as a function of λ and the procedure was repeated for $a = 4.5$, 5.5, and 6.5 fm (Fig. 7). To calculate $\mathcal{L}$, the $\mathcal{R}$-matrix calculations were used together with a normal distribution associated with each experimental data point. The 2σ confidence limits are also displayed as vertical arrows and the $n\sigma$ confidence intervals are obtained by solving $\ln(\mathcal{L}(\lambda)) = \ln(\mathcal{L}_{\max}) - n^2/2$. Figure 7(top) compares $\mathcal{R}$-matrix calculations with present and previous experimental data together while Fig. 7 (bottom) compares the calculations with only previous data sets. The impact of our low-energy measurements clearly shows up and one case of interference $(+\,+\,+)$ can be excluded at the 2σ level for $a = 4.5$ and 5.5 fm. It may also be seen that in the case of a dominant contribution from the $E_r = 38$ keV resonance (small λ), and independent of a, two cases of interference $[(+\,-\,+)$ and $(+\,+\,-)]$ are favored at the 1σ level. This would indicate that for these scenarii the data are insensitive to the sign of the interference between the $E_r = 8$ and 38 keV resonances. However, the data would support constructive interference between the $E_r = 38$ and 665 keV resonances. In the case of a dominant contribution from the $E_r = 8$ keV resonance (large λ), and independent of a, two cases of interference $[(+\,-\,-)$ and $(+\,+\,-)]$ could be favored at the 1σ level. With the existing experimental data the interpretation of the ^{18}F$(p,\alpha)^{15}$O reaction in terms of interference effects is a complex task and definitive conclusions are still difficult to give. Direct measurements at lower energies would help to clarify the situation.

Another interference study concerning the $3/2^+$ levels in the ^{18}F$(p,\alpha)^{15}$O reaction was performed in the past [24]. In that work, the cross section above $E_{\text{c.m.}} = 700$ keV was measured at four energies with the goal of constraining interferences between the $E_r = 8$, 38, and 665 keV resonances. The $\mathcal{R}$-matrix analysis showed that among the interference possibilities between these three resonances the cases with a negative relative sign for the $E_r = 665$ keV resonance term were rejected. Surprisingly the authors of Ref. [24] consider eight different sets of interference signs, whereas only four possibilities are allowed. Moreover, considering the small total widths of the $E_r = 8$ and 38 keV resonances, it is extremely difficult to understand how measurements above the $E_r = 665$ keV resonance can be used to constraint interference effects below $E_{\text{c.m.}} = 500$ keV. A comparison between the two $\mathcal{R}$-matrix analysis is therefore not possible.

V. CONCLUSION

New direct measurements of the ^{18}F$(p,\alpha)^{15}$O cross section at low center-of-mass energies have been reported here. The measurements were made at four different energies and analysed, together with previous existing data, using an $\mathcal{R}$-matrix approach with the aim of constraining the interference effects between the $3/2^+$ resonances in ^{19}Ne which are believed to play an important role in novae nucleosynthesis. The effect of the relative contribution of the two low-lying resonances as well as the sensitivity of the calculations to the $\mathcal{R}$-matrix radius have been investigated in a detailed analysis showing the complexity of the ^{18}F$(p,\alpha)^{15}$O reaction especially when destructive interferences are involved at low center-of-mass energies. This study also showed the importance of performing measurements at low energies even if definite conclusions concerning the interference pattern are still difficult to give. In order to reduce significantly the remaining uncertainties in the ^{18}F$(p,\alpha)^{15}$O reaction rate, more experimental work is still needed. In particular, direct measurements of the cross section at very low center-of-mass energies is of special interest. This should also be complemented by determining the relative contribution of the two low-lying $3/2^+$ resonances as well as their proton widths.

ACKNOWLEDGMENTS

This work was supported by the Belgian IAP program P5/07 on interuniversity attraction poles of the Belgian-State Federal Services for Scientific, Technical and Cultural Affairs and by the European Commission within the 6th Framework Programme through I3-EURONS (Contract

No. RII3-CT-2004-506065). The authors from the universities of Edinburgh and York would like to acknowledge the support of the U.K. Engineering and Physical Sciences Research Council (EPSRC). The continued support of the staff of the LLN cyclotron and the PET group at UCL is gratefully acknowledged.

[1] J. Gómez-Gomar, M. Hernanz, J. Josó, and J. Isern, Mon. Not. R. Astron. Soc. **296**, 913 (1998).
[2] M. Hernanz, J. José, A. Coc, J. Gómez-Gomar, and J. Isern, Astrophys. J. **526**, L97 (1999).
[3] A. Coc, M. Hernanz, J. José, and J.-P. Thibaud, Astron. Astrophys. **357**, 561 (2000).
[4] R. Coszach, M. Cogneau, C. R. Bain, F. Binon, T. Davinson, P. Decrock, T. Delbar, M. Gaelens, W. Galster, J. Görres *et al*., Phys. Lett. **B353**, 184 (1995).
[5] J.-S. Graulich, F. Binon, W. Bradfield-Smith, M. Cogneau, R. Coszach, T. Davinson, T. Delbar, M. Gaelens, W. Galster, J. Görres *et al*., Nucl. Phys. **A626**, 751 (1997).
[6] S. Utku, J. G. Ross, N. P. T. Bateman, D. W. Bardayan, A. A. Chen, J. Görres, A. J. Howard, C. Iliadis, P. D. Parker, M. S. Smith *et al*., Phys. Rev. C **57**, 2731 (1998).
[7] J.-S. Graulich, S. Cherubini, R. Coszach, S. El Hajjami, W. Galster, P. Leleux, W. Bradfield-Smith, T. Davinson, A. di Pietro, A. C. Shotter *et al*., Phys. Rev. C **63**, 011302(R) (2001).
[8] D. W. Bardayan, J. C. Blackmon, W. Bradfield-Smith, C. R. Brune, A. E. Champagne, T. Davinson, B. A. Johnson, R. L. Kozub, C. S. Lee, R. Lewis *et al*., Phys. Rev. C **63**, 065802 (2001).
[9] D. W. Visser, J. A. Caggiano, R. Lewis, W. B. Handler, A. Parikh, and P. D. Parker, Phys. Rev. C **69**, 048801 (2004).
[10] N. de Séréville, A. Coc, C. Angulo, M. Assuncao, D. Beaumel, B. Bouzid, S. Cherubini, M. Couder, P. Demaret, F. de Oliveira Santos *et al*., Phys. Rev. C **67**, 052801(R) (2003).
[11] R. L. Kozub, D. W. Bardayan, J. C. Batchelder, J. C. Blackmon, C. R. Brune, A. E. Champagne, J. A. Cizewski, T. Davinson, U. Greife, C. J. Gross *et al*., Phys. Rev. C **71**, 032801(R) (2005).
[12] N. de Séréville, E. Berthoumieux, and A. Coc, Nucl. Phys. **A758**, 745c (2005).
[13] M. Cogneau, P. Decrock, M. Gaelens, D. Labar, P. Leleux, M. Loiselet, and G. Ryckewaert, Nucl. Instrum. Methods A **420**, 489 (1999).
[14] T. Davinson, W. Bradfield-Smith, S. Cherubini, A. di Pietro, W. Galster, A. M. Laird, P. Leleux, A. Ninane, A. N. Ostrowski, A. C. Shotter *et al*., Nucl. Instrum. Methods A **454**, 350 (2000).
[15] N. de Séréville, A. Coc, C. Angulo, M. Assuncao, D. Beaumel, B. Bouzid, S. Cherubini, M. Couder, P. Demaret, F. de Oliveira Santos *et al*., Eur. Phys. J. Special Topics **150**, 211 (2007).
[16] H. Lorenz-Wirzba, P. Schmalbrock, H. P. Trautvetter, M. Wiescher, C. Rolfs, and W. S. Rodney, Nucl. Phys. **A313**, 346 (1979).
[17] N. S. Christensen, F. Jensen, F. Besenbacher, and I. Stensgaard, Nucl. Instrum. Methods B **51**, 97 (1990).
[18] D. W. Bardayan, J. C. Batchelder, J. C. Blackmon, A. E. Champagne, T. Davinson, R. Fitzgerald, W. R. Hix, C. Iliadis, R. L. Kozub, Z. Ma *et al*., Phys. Rev. Lett. **89**, 262501 (2002).
[19] A. M. Lane and R. G. Thomas, Rev. Mod. Phys. **30**, 257 (1958).
[20] M. Dufour and P. Descouvemont, Nucl. Phys. **A785**, 381 (2007).
[21] J. C. Dalouzy (private communication).
[22] N. de Séréville, A. Coc, C. Angulo, M. Assuncao, D. Beaumel, B. Bouzid, S. Cherubini, M. Couder, P. Demaret, F. de Oliveira Santos *et al*., Nucl. Phys. **A791**, 251 (2007).
[23] D. W. Bardayan, J. C. Blackmon, J. Gómez del Campo, R. L. Kozub, J. F. Liang, Z. Ma, L. Sahin, D. Shapira, and M. S. Smith, Phys. Rev. C **70**, 015804 (2004).
[24] K. Y. Chae, D. W. Bardayan, J. C. Blackmon, D. Gregori, M. W. Guidry, M. S. Johnson, R. L. Kozub, R. J. Livesay, Z. Ma, C. D. Nesaraja *et al*., Phys. Rev. C **74**, 012801(R) (2006).